RESEARCH ARTICLE | SEPTEMBER 01 2023

Nonlinear optical response of anthracene as a D-π-A conjugated system: Quantum computation study

S. Resan; R. Hameed; F. Bahrani; M. Al-Anber

AIP Conference Proceedings 2806, 050007 (2023)
https://doi.org/10.1063/5.0163185

Nonlinear Optical Response of Anthracene as a D-π-A Conjugated System: Quantum Computation Study

S. Resan[a], R. Hameed[a], F. Bahrani[a] And M. Al-anber[a]

[a]*Molecular Engineering and Computational Modeling Lab, Department of Physics, College of Science, University of Basrah, Basrah, Iraq.*

Corresponding author: *samira.resan@uobasrah.edu.iq*

Abstract. Quantum parameters of the nonlinear optics, in general, depend on selecting the donor-acceptor sites with anthracene. In this investigation, the dipole moment, polarizability, anisotropy of the polarizability and first-order were investigated using the Density Functional Theory (DFT/B3LYP/6-311G(d,p)). Also, the highest occupied molecular orbital energy level (E_{HOMO}), the lowest unoccupied molecular orbital energy level (E_{LUMO}), and the HOMO-LUMO energy gap (E_g) were studied. This study shows that the two structures ($D_{10}A_5$ and $D_{10}A_4$) have a large hyperpolarizability and would have possible utilization for the advancement of nonlinear optics devices.

Keywords: Anthracene, Nonlinear optics, Charge transfer, Electro-optical properties.

INTRODUCTION

The large second-order nonlinear optical (NLO) properties due to the substituted organic molecules (Donor-acceptor) have been utilised in various research applications because of their potential applicability in many fields, like frequency doubling, optoelectronics[1], optical modulation, optical data processing, molecular switching[2,3], organic light-emitting diodes (OLEDs) [4], data storage and high-speed optical communications (HSOC). An essential objective in developing nonlinear optical utilization is to obtain highly energetic substances with large second-order polarizabilities. Generally, the second-order polarizability response is associated with an intramolecular charge transfer (ICT) within the donor- bridge- acceptor system. Both kinds of research (theoretical and experimental) have determined that high hyperpolarizabilities usually result from the incorporation of a potent electron donor and acceptor located at opposite ends of a decorous molecular conjugation route (Fig. 1), which is a π-bridge [3,6–10].

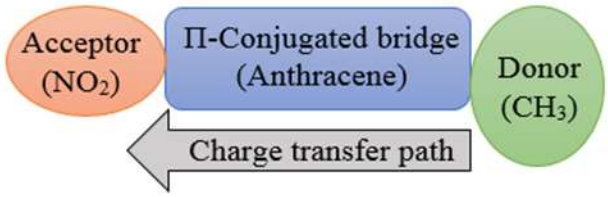

FIGURE 1. The Schematic illustrated a nonlinear push-pull anthracene as a π-conjugation path.

Many donor-acceptor organic molecules have been reported previously[20–22,12–19]. Their structure-property correlation reveals that the hyperpolarizability grows through an increased path length of π-bridge[239]. The experimental and theoretical researches have pointed out that the styling of substances including huge second-order (NLO) characteristics should essentially be concentrated on the planar of donor-conjugated bridge-acceptor forms, bond length alternation structure (BLAS)[24,25] heterocyclic donor groups and acceptors[24,26–28], and twisted π-electron[29] structures [30–32]. Usually, the more potent the donor group, which depends on the difference between the ground and excited states, and the shorter the frequency of the UV-visible absorption. This redshift implies an improvement in the

2nd Muthanna International Conference on Engineering Science and Technology
AIP Conf. Proc. 2806, 050007-1–050007-8; https://doi.org/10.1063/5.0163185
Published by AIP Publishing. 978-0-7354-4629-8/$30.00

hyperpolarizability of the donor-bridge-acceptor, according to NLO investigations[33]. Most researchers have reported the best donor and acceptor groups in their researches, regardless if these groups enhanced the hyperpolarizability directly or by making some changes in the geometry of the π-bridge. Many reports focused on the side group (s) substitution strategy to enhance the nonlinear optical properties [34–37]. Also, on the correspondence between the hyperpolarizabilities and the energy band gaps [35,36,38], while very few publications have been focused on determining the influence of the rotation around the central axis of the nonlinear optical molecules [38–41] Nevertheless, more computational data of nonlinear optical behaviour for different materials are required. In particular, it would seem desirable to evaluate the nonlinear optical responses of nanotubes according to their dimensions [42,43] and fullerenes [42,43]. In addition, the nonlinear optical behaviour of nanotubes has been used in anti-cancer drugs [44,45]. In this study, we investigated the influence of donor and acceptor groups' positions on anthracene by choosing various positions, as shown in Fig. 2, to enhance hyperpolarizability.

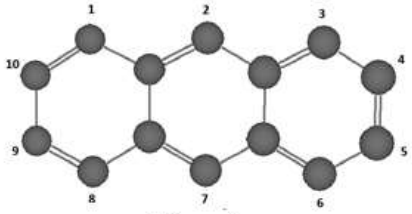

D_k-π-A_n
where k=1 or 10 while n=1,2…10 so tha k≠n
D_k=CH_3, π = Anthracene and A_n=NO_2

FIGURE 2. The numbering scheme is used for the variation in functional groups D and A positions around anthracene (D_k-π-A_n).

THEORY AND METHODS OF CALCULATION

The charge density of the molecule may be reset when they are topic to an external electric field, ϵ, and then the dipole moment may turn. This variation of the dipole moment, μ_i, can be expressed as the first derivative of the total molecular energy, E, to the electric field component (ϵ_i) in symbols [34,35]:

$$\mu_i = (\delta E/\delta \epsilon_i)_{\epsilon=0} \quad (1)$$

As well as, the second derivative of the total molecular energy, E, to the electric field component (ϵ_i); provides the polarizability in form [3435]:

$$\alpha_{ij} = (\delta^2 E/\delta \epsilon_i \delta \epsilon_i)_{(\epsilon=0)} \quad (2)$$

The mean static polarizability $< \alpha >$ is represented as:

$$< \alpha > = (1/3)(\alpha_{xx} + \alpha_{yy} + \alpha_{zz}) \quad (3)$$

where the diagonal elements of the polarizability matrix are α_{xx}, α_{yy}, and α_{zz} [46,47]. The anisotropic polarizability ($\Delta\alpha$) is ordinarily defined as [38,46]:

$$\Delta\alpha = (1/2)\,[(\alpha_{xx} - \alpha_{yy})^2 + (\alpha_{yy} - \alpha_{zz})^2 + (\alpha_{zz} - \alpha_{xx})^2]^{1/2} \quad (4)$$

The anisotropy (k) is the measurement of deviations from the spherical charge symmetry that would be zero when the total charge distribution be spherically [34]; in symbols:

$$k = \alpha_{xx}^2 + \alpha_{yy}^2 + \alpha_{zz}^2 - 3 < \alpha >^2)/(6 < \alpha >^2) \quad (5)$$

The molecular hyperpolarizability is defined as:

$$\beta_{ijk} = (\delta^3 E/\delta\epsilon_i \delta\epsilon_j \delta\epsilon_k)_{(\epsilon=0)} \quad (6)$$

The output of GAUSSIAN-09W version gives ten components from the matrix of hyperpolarizability, in atomic units (a.u), as $\beta_{xxx}; \beta_{xxy}; \beta_{xyy}; \beta_{yyy}; \beta_{xzz}; \beta_{xyz}; \beta_{yyz}; \beta_{xzz}; \beta_{yzz}; \beta_{zzz}$, so that:

$$\beta_{tot} = [\beta_x^2 + \beta_y^2 + \beta_z^2]^{1/2} \quad (7)$$

Where $\beta_x = (\beta_{xxx} + \beta_{xyy} + \beta_{xzz})$, $\beta_y = (\beta_{yyy} + \beta_{yzz} + \beta_{yxx})$ and $\beta_z = (\beta_{zzz} + \beta_{zxx} + \beta_{zyy})$ respectively [38,46]. The molecular hyperpolarizability (β_{tot}) along the direction of the electric dipole moment, is described by β_μ, which is represented as [38,47]:

$$\beta_\mu = (\mu_x\beta_x + \mu_y\beta_y + \mu_z\beta_z)/\mu \quad (8)$$

The measuring of hyperpolarizability in the XY-plane of the molecular structure ($\beta_{xy-\text{plane}}$) is given as [29]:

$$\beta_{xy-\text{plane}} = (\beta_{xxx} + \beta_{xxy} + \beta_{yyy}) \quad (9)$$

How do changes in the molecular structure can lead to variations in the measured β_{tot} values? For this purpose, from the complex sum-over-states (SOS) illustration, the two-state model that exposes the low-lying charge-transfer transition (CT) has been investigated. In this state, the relationship:

$$\beta_\circ = (\Delta\mu f_\circ/\Delta E^{*3}) \quad (10)$$

can be used to note the CT [29,48,49], where Δμ is the transition dipole moment, ΔE^* is the transition energy, and $f_\circ$ is the oscillator strength. We adopted the anthracene molecule as π-bridge for the D-π-A system because it is a strong planar against molecular resistance to any probable torsion by the donor-acceptor groups. The CH_3 and NO_2 were adopted as the donor and acceptor, respectively, for different positions around the anthracene so that we can get 18 D-π-A isomers, see Fig. 3. We limited the donor group around two positions only, according to the numbering: D_kA_n= (D_k-π-A_n), where k=1 or 10 while n=1,2…10 so that k≠n. The extended basis sets are required to accurately calculate the dipole moment, static polarizability and first static hyperpolarizability. A split-valence triple-zeta basis 6-311G (d,p), which is a Pople-type basis, adds one set of *d* functions to heavy atoms plus *p* polarisation functions for hydrogen [50,51]. Full optimisation of these 18 cases was carried out using B3LYP with a 6-311G(d,p) basis set, commonly approved as a helpful plan to estimate the molecular structures. The B3LYP is an aggregate of Becke's three-parameter hybrid exchange functional (B3) with the Lee-Yang-Parr correlation functional (LYP) [52,53]. UV-Vis analysis was calculated utilizing time-dependent density functional theory (TD-DFT) with B3LYP level and 6-311G(d,p) basis sets. The B3LYP functional is regularly regarded as a gateway option to prognosticate the NLO characteristics of small molecules[47]. Whole theoretical computations were done by the Gaussian 09 program package utilising density functional theory (DFT) [46]. Furthermore, the input files were organised utilising Gauss View 5.0 [54].which was also utilised to interpret the output files issues.

RESULTS AND DISCUSSION

For our study, it was essential to exam the most stable ΔE (relative energy), which is the difference among the total energies due to the highest one, isomers of the D-π-A anthracene, see Table 1. Among the 18 possible isomers, there were three from the most stable configurations of the anthracene derivatives, as shown in Fig. 4. Moreover, it was found that the $D_{10}A_5$ was favoured over the $D_{10}A_4$ and D_1A_9 ones by ΔE=0.104 and ΔE=0.853 kcal/mol, respectively, employing the method of B3LYP with basis set 6-311G(d,p). According to the available literature, there are no experimental data for the studied compounds for comparison.

FIGURE 3. The optimised molecules were got utilising B3LYP/6-311G(d,p) of the most stable (ΔE) isomers of the D-π-A conjugated system ($D_{10}A_5$, $D_{10}A_4$ and D_1A_9.

The highest occupied and the lowest unoccupied molecular orbital, HOMO and LUMO, have identified frontier orbitals that lie at the outside limits of the molecule's electrons. The estimated values for the E_{LUMO} and E_{HOMO} and the energy gap (E_g), $E_g = E_{HOMO} - E_{LUMO}$, for various positions of the acceptor and donor have been given in Table 2. ELUMO indicates its ability to accept electrons, while E_{HOMO} is often connected with the ability of electron-donating [56]. D_1A_2 and $D_{10}A_1$ have the lowest E_{HOMO} values compared to the other derivatives, so they have the highest electron-donating ability. On the other hand, D_1A_4, D_1A_6, D_1A_3, and D_1A_5 have the highest E_{LUMO} values in decreasing order, so it was expected that they would have the highest electron-accepting ability, see Table 3.

TABLE 1. B3LYP with basis set 6-311G(d,p) estimated relative energy ΔE (in kcal/mol), energy levels of the LUMO, HOMO and (E_{HOMO}-E_{LUMO}) the energy gap (in eV) for the various positions of D and A.

Positions	ΔE	E_{HOMO}	E_{LUMO}	E_g
D_1A_2	12.832	-5.865	-2.369	3.496
D_1A_3	5.138	-5.907	-2.789	3.119
D_1A_4	1.082	-5.992	-2.798	3.195
D_1A_5	1.091	-5.991	-2.7868	3.205
D_1A_6	5.259	-5.916	-2.790	3.127
D_1A_7	8.850	-5.951	-2.620	3.332
D_1A_8	5.011	-5.939	-2.745	3.195
D_1A_9	0.853	-6.007	-2.775	3.232
D_1A_{10}	5.540	-5.974	-2.674	3.300
$D_{10}A_1$	6.669	-5.869	-2.564	3.306
$D_{10}A_2$	7.528	-5.943	-2.595	3.349
$D_{10}A_3$	4.224	-5.907	-2.749	3.158
$D_{10}A_4$	0.104	-5.981	-2.763	3.218
$D_{10}A_5$	0.000	-5.986	-2.749	3.238
$D_{10}A_6$	4.253	-5.909	-2.752	3.158
$D_{10}A_7$	7.584	-5.942	-2.614	3.329
$D_{10}A_8$	4.276	-5.901	-2.744	3.157
$D_{10}A_9$	3.464	-5.944	-2.737	3.207

The molecular dipole moment is a significant characteristic, where it has mainly explained the intermolecular interactions that require the non-bonded model dipole-dipole interactions. That is due to the more significant the dipole moment, the more robust the interactions among the molecules [55]. The studied anthracene derivatives have been the dipole moments got utilising DFT computations are summarised in Table 4. The dipole moments in the issues of $D_{10}A_5$ (μ = 6.552 a.u), $D_{10}A_4$ (μ = 6.434 a.u), and D_1A_5 (μ = 6.0857 a.u) has higher rates utilising B3LYP with basis set 6-311G (d,p) are at most associated to an aggregate asymmetry in the charge from the donator group during the π-bridge to the acceptor group. Generally, the longitude dipole component (μ_x) along the molecular axis was dominant.

Another important feature of a molecule's electronic properties is its polarizability. Analysis values of the polarizability are listed in Table 5; the values range from $< \alpha >$ = 99.1868 a.u to $< \alpha >$ =107.1654 a.u. D_1A_5 ($< \alpha >$ =107.1654 a.u), $D_{10}A_5$ ($< \alpha >$ =106.7378 a.u), D_1A_4 ($< \alpha >$ =106.723 a.u) and $D_{10}A_4$ ($< \alpha >$ =106.496 a.u) had the highest values, respectively. The values of transverse static polarizabilities (α_{zz}) are very high compared to the α_{yy}.

And, in some cases, to the longitudinal polarizability (α_{xx}). For the researchers who used the same donor-acceptor group with other π-bridges, the α_{zz} dipole component was still lower than the longitudinal polarizability [34,35]. The σ-bonds of the CH_3 group will provide the polarizability in a path perpendicular to the plane. Nevertheless, the π-electrons maybe contribute to the polarizability via π-bonds (in the case of anthracene). Table 6 shows the anisotropic polarizability Δα, which relies on the electric field's direction, being significantly smaller than the average polarizability $< \alpha >$. $D_{10}A_3$ ($\Delta\alpha$ = 26.963 a.u), D_1A_4 ($\Delta\alpha$ = 26.097 a.u), $D_{10}A_6$ ($\Delta\alpha$ = 26.032 a.u), $D_{10}A_7$ ($\Delta\alpha$ = 25.86355), $D_{10}A_8$ ($\Delta\alpha$ = 25.735 a.u), and $D_{10}A_2$ ($\Delta\alpha$ = 25.721 a.u) had, the decreasing order, the highest anisotropic polarizability. That means they have the lowest perpendicular polarizability to the symmetry axes of the molecule compared to the parallel polarizability. Therefore, the polarizability along anthracene's axis was higher than the same donor-acceptor group used with trans-hexatriene (NO_2–$(CH,CH)_3$–CH_3) [35]. Table 7 illustrates that D_1A_8 (κ =0.000961), D_1A_3 (κ =0.001114), D_1A_6 (κ =0.001244) and $D_{10}A_3$ (κ =0.001521) had the lowest deviations from spherical symmetry. Thus, D_1A_8 had the highest spherically symmetric charge distribution. Furthermore, all anthracene's isomers had very low anisotropy results compared with the results of the polyacetylene chain (NO_2-$(CH,CH)_4$–CH_3), which used the same donator and acceptor groups [34]. Thus, anthracene's isomers had the highest spherically symmetric charge distribution compared with the polyacetylene chain. Where it maybe shows the idea that the shape of molecules that are used as the π-bridge also has a big role in enhance of the NLO properties.

TABLE 2. B3LYP with basis set 6-311G(d,p) estimated dipole moment, main polarizability tensor, polarizability, anisotropic polarizability (in a.u) and anisotropy for the various positions of D and A.

Positions	μ	μ_x	α_{xx}	α_{yy}	α_{zz}	$< \alpha >$	$\Delta\alpha$	K
D_1A_2	3.535	-0.124	-84.269	-102.322	-112.070	99.554	24.440	0.0066
D_1A_3	4.440	2.488	-98.197	-98.056	-108.289	101.514	24.911	0.0011
D_1A_4	5.836	5.688	-119.010	-93.792	-107.368	106.723	26.097	0.0046
D_1A_5	6.086	-5.982	-120.846	-93.274	-107.376	107.165	24.692	0.0055
D_1A_6	5.192	3.653	-103.282	-95.828	-108.267	102.459	23.316	0.0012
D_1A_7	4.642	1.375	-86.787	-104.058	-110.610	100.485	23.303	0.005
D_1A_8	5.269	2.723	-98.243	-99.527	-108.309	102.026	24.734	0.0009
D_1A_9	5.935	-5.633	-116.824	-93.881	-107.363	106.023	24.728	0.0039
D_1A_{10}	5.2905	5.281	-116.434	-91.286	-108.799	105.506	23.081	0.0049
$D_{10}A_1$	4.029	-1.592	-90.763	-99.414	-110.120	100.099	24.907	0.0031
$D_{10}A_2$	4.250	0.392	-82.603	-104.496	-110.462	99.187	25.721	0.0072
$D_{10}A_3$	4.992	2.994	-94.695	-100.356	-108.291	101.114	26.963	0.0015
$D_{10}A_4$	6.434	6.242	-117.263	-94.861	-107.363	106.496	24.490	0.0037
$D_{10}A_5$	6.552	6.468	-118.794	-94.058	-107.362	106.738	23.556	0.0044
$D_{10}A_6$	5.148	-3.634	-98.752	-97.880	-108.318	101.650	26.032	0.0010
$D_{10}A_7$	4.475	1.438	-83.803	-104.983	-110.404	99.730	25.864	0.0066
$D_{10}A_8$	4.741	-1.567	-92.115	-103.141	-108.261	101.172	25.735	0.0022
$D_{10}A_9$	5.148	-4.752	-110.834	-95.282	-108.081	104.732	22.390	0.0020

$D_{10}A_5$ (β_{tot}=200.506 a.u), $D_{10}A_4$ (β_{tot}=191.006 a.u), D_1A_5 (β_{tot}=169.844 a.u), D_1A_4 (β_{tot}=156.766 a.u) and D_1A_9 (β_{tot}=149.490 a.u) produced the highest enhancements, in decreasing order, of the first hyperpolarizability, as illustrated in Table 8. In all these cases, the β_x was dominant. Perhaps, the longest distances between the donor group and acceptor group give the highest static hyperpolarizability. Nevertheless, surprisingly the shortest distances between the donor and acceptor (one bond length) also had high static hyperpolarizability, as with D_1A_{10} (β_{tot}=133.953 a.u) and $D_{10}A_9$ (β_{tot}=122.793 a.u). All molecular structures under study were characterised by quasi-parallel dipole moment (μ) and hyperpolarizability (β_{tot}), as shown through the β_μ results in Table 9. Consequently, all the β_μ values have been positive, and there were no interesting variations in the corresponding orientation of the dipole moment regarding the molecular structures. Indeed, though the larger hyperpolarizability (β_{tot}) values are commonly correlated with the higher β_μ amounts, this issue from the range of π-bridge furthermore at the tensor level is connected by a heavily aggressive $\beta_\circ$ value, see Table 10, where the $\beta_\circ$ was calculated from $\beta_\circ = \beta_\circ^1 + \beta_\circ^2 + \beta_\circ^3$; where $\beta_\circ^1$, $\beta_\circ^2$ and $\beta_\circ^3$ were calculated due to the first, second, and third singlet excitations. The change in the value of $\beta_\circ$ too depends on the changes in the transition moment of the substrate. As the molecule has a more significant difference of transition moment, the charge transfer (CT) is more open, and the dipole moment's value is higher. $D_{10}A_5$

had been the highest values of both β_{tot} and β_o. Moreover, according to our results, there was no synchronisation between β_{tot} and β_o for most cases. Table 11 tells that the highest amounts of the $\beta_{xy-\text{plane}}$ corresponded to high amounts of β_{tot}. Because the D-π-A lies in the XY plane, and the X-axis is directed adjacent to the molecular charge transfer (CT) axis, the isomers have got both the highest β_{tot} and the most significant component of the hyperpolarizability (β_{xxx}). At the same time, every other hyperpolarizability components were small. As a result, the total hyperpolarizability can be achieved by the interpretation: $\beta_{tot} \sim \beta_{xxx}$. A method to evaluate better the nonlinear optics (NLO) sense, the "in-plane nonlinear anisotropy" thought u (relying on the rate $u = \beta_{xxy}/\beta_{yyy}$), was introduced in this work.

TABLE 3. B3LYP with basis set 6-311G(d,p) estimated hyperpolarizability components (a.u) and nonlinear anisotropy for the various positions of D and A.

Positions	β_x	β_y	β_z	β_{tot}	β_μ	$B_{xy\text{-plane}}$	β_o	U
D_1A_2	-8.281	-19.189	0.003	20.900	19.467	49.761	48.799	0.183
D_1A_3	31.364	-46.401	6.590	56.393	55.959	106.601	72.026	1.475
D_1A_4	153.745	-30.629	0.005	156.766	156.699	220.411	118.971	2.247
D_1A_5	-168.874	18.128	0.021	169.844	169.331	214.519	59.262	108.730
D_1A_6	59.019	45.593	6.234	74.839	73.902	126.131	109.415	3.889
D_1A_7	6.426	-34.016	-0.651	34.624	34.394	62.153	98.002	0.134
D_1A_8	48.020	51.441	5.029	70.550	68.810	123.502	77.779	1.140
D_1A_9	-146.246	30.973	0.003	149.490	148.557	209.133	108.974	5.036
D_1A_{10}	133.624	8.947	2.826	133.953	133.860	171.274	78.110	1.604
$D_{10}A_1$	-13.383	32.491	-5.182	35.520	35.090	68.431	68.304	1.275
$D_{10}A_2$	2.445	-26.493	-1.337	26.639	26.601	41.813	97.360	0.043
$D_{10}A_3$	50.339	51.474	-6.755	72.313	71.326	125.972	113.428	1.421
$D_{10}A_4$	187.850	34.582	-0.011	191.006	190.628	253.924	73.513	2.900
$D_{10}A_5$	199.259	22.323	0.034	200.506	200.270	249.749	134.005	4.798
$D_{10}A_6$	-66.099	49.248	-6.912	82.718	81.514	137.891	83.496	2.371
$D_{10}A_7$	11.526	-32.473	-1.410	34.486	34.456	50.578	131.929	0.104
$D_{10}A_8$	-28.395	-50.254	4.589	57.904	56.788	108.685	107.155	0.974
$D_{10}A_9$	-117.507	35.454	-3.658	122.793	122.151	186.739	120.540	8.850

The nonlinear anisotropy (u) values have been recorded in Table 12 and the results identify considerable large values for D_1A_5 (u=108.735), $D_{10}A_9$ (u=8.850), D_1A_9 (u= 5.036), $D_{10}A_5$ (u=4.798), D_1A_6 (u=3.889), which demonstrates that our structures possessed good 2D second-order nonlinear optics (NLO) characteristics. The different positions of donor/acceptor groups will change both the LUMO and HOMO energies considerably, and perhaps this has pointed to a higher/less energy gap and given a decrease/increase in β_{tot} value. It does not clearly show the inverse proportion by the energy gap that has been published in many previously reported about this matter [34,35]. It seems the NLO properties are sensitive to donator-acceptor positions. The stability, electric dipole moment, and hyperpolarizability utilities for $D_{10}A_5$ and $D_{10}A_4$ were more significant than the other isomers. The B3LYP with the basis set 6-311G(d,p) estimated β_{tot} and ΔE values for chosen isomers point that it would be attractive to synthesise aggregates as $D_{10}A_5$ and $D_{10}A_4$ having the greatest hyperpolarizability and stability values, respectively. The investigation shows that the $D_{10}A_5$ and $D_{10}A_4$ have high hyperpolarizability and the potential to develop nonlinear optics (NLO) materials. The examination of the hyperpolarizability has been demonstrated by the calculating of the frontier orbital energies. That encourages adopting intramolecular charge transfer (CI) to describe the static hyperpolarizability. Consequently, early estimations determined the opposite relation between hyperpolarizability and energy gaps [33,55].

CONCLUSION

The D-π-A structures and quantum molecular parameters of various anthracene isomers were studied by the B3LYP with basis set 6-311G(d,p). The nonlinear optical response was examined by defining the dipole moment, polarizability and static hyperpolarizability. This study showed that the $D_{10}A_5$ and $D_{10}A_4$ structures have valuable hyperpolarizabilities and possibly develop nonlinear optics (NLO) substances.

REFERENCES

[1] F.Z. Henari, D. Gaynor, D.M. Griffith, C. Mulcahy, and C.J. Marmion, Chem. Phys. Lett. **552**, 126 (2012).
[2] L.T. Cheng, W. Tam, S.R. Marder, A.E. Stiegman, G. Rikken, and C.W. Spangler, J. Phys. Chem. **95**, 10643 (1991).
[3] M.R.S.A. Janjua, W. Guan, L. Yan, Z.M. Su, M. Ali, and I.H. Bukhari, J. Mol. Graph. Model. **28**, 735 (2010).
[4] M. Jagadeesh, M. Lavanya, S.K. Kalangi, Y. Sarala, C. Ramachandraiah, and A. Varada Reddy, Spectrochim. Acta - Part A Mol. Biomol. Spectrosc. **135**, 180 (2015).
[5] K.D. Belfield, K.J. Schafer, Y. Liu, J. Liu, X. Ren, and E.W. Van Stryland, J. Phys. Org. Chem. **13**, 837 (2000).
[6] A. Merouane, A. Mostefai, D. Hadji, A. Rahmouni, M. Bouchekara, A. Ramdani, and S. Taleb, Monatshefte Fur Chemie **151**, 1095 (2020).
[7] M.R.S.A. Janjua, J. Iran. Chem. Soc. **14**, 2041 (2017).
[8] M. Khalid, A. Ali, A.F. De la Torre, K.P. Marrugo, O. Concepcion, G.M. Kamal, S. Muhammad, and A.G. Al-Sehemi, ChemistrySelect **5**, 2994 (2020).
[9] M.R.S.A. Janjua, S. Jamil, T. Ahmad, Z. Yang, A. Mahmood, and S. Pan, Comput. Theor. Chem. **1033**, 6 (2014).
[10] M.R.S.A. Janjua, Inorg. Chem. **51**, 11306 (2012).
[11] V. Keshari, S.P. Karna, and P.N. Prasad, J. Phys. Chem. **97**, 3525 (1993).
[12] S. Altürk, N. Boukabcha, N. Benhalima, Ö. Tamer, A. Chouaih, D. Avcı, Y. Atalay, and F. Hamzaoui, Indian J. Phys. **91**, 501 (2017).
[13] M.R.S.A. Janjua, Z.M. Su, W. Guan, C.G. Liu, L.K. Yan, P. Song, and G. Maheen, Aust. J. Chem. **63**, 836 (2010).
[14] F.Y. Li, J. Zheng, L.P. Jin, X.S. Zhao, T.T. Liu, and J.Q. Guo, J. Mater. Chem. **10**, 1287 (2000).
[15] S. Barlow, H.E. Bunting, C. Ringham, J.C. Green, G.U. Bublitz, S.G. Boxer, J.W. Perry, and S.R. Marder, J. Am. Chem. Soc. **121**, 3715 (1999).
[16] S.S.P. Chou, G.T. Hsu, and H.C. Lin, Tetrahedron Lett. **40**, 2157 (1999).
[17] H.E. Katz, K.D. Singer, J.E. Sohn, C.W. Dirk, L.A. King, and H.M. Gordon, J. Am. Chem. Soc. **109**, 6561 (1987).
[18] A.O. Adeloye and P.A. Ajibade, *Towards the Development of Functionalized Polypyridine Ligands for Ru(II) Complexes as Photosensitizers in Dye-Sensitized Solar Cells (DSSCs)* (2014).
[19] B.R. Cho, K.N. Son, S.J. Lee, T.I. Kang, and M.S. Han, **39**, 3167 (1998).
[20] M. Chandrasekharam, G. Rajkumar, T. Suresh, C.S. Rao, P.Y. Reddy, J.H. Yum, M.K. Nazeeruddin, and M. Graetzel, Adv. Optoelectron. **2011**, 22 (2011).
[21] S.S. Sun, C. Zhang, L.R. Dalton, S.M. Garner, A. Chen, and W.H. Steier, Chem. Mater. **8**, 2401 (1996).
[22] M. Ahlheim, M. Barzoukas, P. V Bedworth, M. Blanchard-, A. Fort, Z. Hu, S.R. Marder, J.W. Perry, C. Runser, M. Ahiheim, M. Barzoukas, P. V Bedworth, M. Blanchard-desce, A. Fort, Z. Hu, S.R. Marder, J.W. Perry, C. Runser, M. Staehelin, and B. Zysset, (2016).
[23] T. Coradin, J. Mater. Chem. **7**, 853 (1997).
[24] M.R.S.A. Janjua, Open Chem. **15**, 139 (2017).
[25] M. Khalid, R. Jawaria, M.U. Khan, A.A.C. Braga, Z. Shafiq, M. Imran, H.M.A. Zafar, and A. Irfan, ACS Omega **6**, 16058 (2021).
[26] F. Meyers, S.R. Marder, B.M. Pierce, and J.L. Bredas, J. Am. Chem. Soc. **116**, 10703 (1994).
[27] K.D. Belfield, C. Chinna, and K.J. Schafer, Tetrahedron Lett. **38**, 6131 (1997).
[28] E.M. Breitung, C.F. Shu, and R.J. McMahon, J. Am. Chem. Soc. **122**, 1154 (2000).
[29] I.D.L. Albert, T.J. Marks, and M.A. Ratner, J. Am. Chem. Soc. **119**, 6575 (1997).
[30] S. Resan, R. Hameed, A. Al-Hilo, and M. Al-Anber, Rev. Cuba. Fis. **37**, 95 (2020).
[31] H. Kang, A. Facchetti, H. Jiang, E. Cariati, S. Righetto, R. Ugo, C. Zuccaccia, A. Macchioni, C.L. Stern, Z. Liu, S.T. Ho, E.C. Brown, M.A. Ratner, and T.J. Marks, J. Am. Chem. Soc. **129**, 3267 (2007).
[32] X. Meng, B. Li, Z. Chen, L. Yao, D. Zhao, X. Yang, M. He, and Q. Yu, J. Enzyme Inhib. Med. Chem. **22**, 293 (2007).
[33] H. Kang, A. Facchetti, P. Zhu, H. Jiang, Y. Yang, E. Cariati, S. Righetto, R.R.R. Ugo, C. Zuccaccia, A. Macchioni, C.L. Stern, Z. Liu, S.-T.T. Ho, and T.J. Marks, Angew. Chemie **117**, 8136 (2005).
[34] Y.G. Sidir, Y. GÜLSEVEN SIDIR, I. Sidir, I. SIDIR, H. BERBER, H. Berber, E. TAŞAL, and E. Tasal, Bitlis Eren Univ. J. Sci. Technol. **1**, 7 (2015).
[35] N.S. Labidi, Arab. J. Chem. **9**, S1252 (2016).
[36] N.S. Labidi, A. Djebaili, and I. Rouina, J. Saudi Chem. Soc. **15**, 29 (2011).
[37] G. Park, W.S. Jung, and C.S. Ra, Bull. Korean Chem. Soc. **25**, 1427 (2004).
[38] K.S. Thanthiriwatte and K.M. Nalin de Silva, J. Mol. Struct. THEOCHEM **617**, 169 (2002).

[39] N. Abeyasinghe, R. Silva, and K. Silva, Int. Res. J. Pure Appl. Chem. **13**, 1 (2016).
[40] M. Bahat and E. Yörük, Proc. 9th WSEAS Int. Conf. Appl. Comput. Sci. ACS '09 40 (2009).
[41] S.A. Siddiqui, T. Rasheed, M. Faisal, A.K. Pandey, and S.B. Khan, Spectrosc. (New York) **27**, 185 (2012).
[42] H. Alyar, M. Bahat, E. Kasap, and Z. Kantarci, Czechoslov. J. Phys. **56**, 349 (2006).
[43] M.J. Al-anber, Z.S. Abdullah, S.F. Resan, and A.M. Ali, J. Mater. Environ. Sci. **3**, 636 (2012).
[44] A.K. Al-lami and A.M. Ali, Eur. Acad. Res. (2014).
[45] M.J. Al-Anber, Rev. Cuba. Fis. **30**, 72 (2013).
[46] M.J. Al-Anber, A.H. Al-Mowali, and A.M. Ali, Acta Phys. Pol. A **126**, 845 (2014).
[47] M.N. Arshad, A.A.M. Al-Dies, A.M. Asiri, M. Khalid, A.S. Birinji, K.A. Al-Amry, and A.A.C. Braga, J. Mol. Struct. **1141**, 142 (2017).
[48] B. Baroudi, K. Argoub, D. Hadji, A.M. Benkouider, K. Toubal, A. Yahiaoui, and A. Djafri, J. Sulfur Chem. **41**, 310 (2020).
[49] S. Muhammad, A.G. Al-Sehemi, Z. Su, H. Xu, A. Irfan, and A.R. Chaudhry, J. Mol. Graph. Model. **72**, 58 (2017).
[50] M.R.S.A. Janjua, J. Mex. Chem. Soc. **62**, 125 (2018).
[51] G. Uğurlu and H. Necefoğlu, AIP Conf. Proc. **1935**, 2 (2018).
[52] W.J. Hehre, K. Ditchfield, and J.A. Pople, J. Chem. Phys. **56**, 2257 (1972).
[53] A. Migalska-Zalas, K. EL Korchi, and T. Chtouki, Opt. Quantum Electron. **50**, (2018).
[54] H. Alyar, M. Bahat, Z. Kantarci, and E. Kasap, Comput. Theor. Chem. **977**, 22 (2011).
[55] A.B. Nielsen and A.J. Holder, *GaussView. User's Reference* (Gaussian, Incorporated, 1998).
[56] A. Eşme and S. Güneşdoğdu Sağdinç, BAÜ Fen Bil. Enst. Derg. Cilt **16**, 47 (2014).